Canadian Mineralogist
Vol. 16, pp. 611-623 (1978)

STUDIES OF THE SULFOSALTS OF COPPER. VI. LOW-TEMPERATURE EXSOLUTION IN SYNTHETIC TETRAHEDRITE SOLID SOLUTION, $Cu_{12+x}Sb_{4+y}S_{13}$

EMIL MAKOVICKY
Institute of Mineralogy, University of Copenhagen, Østervoldgade 7–5, DK–1350 Copenhagen K, Denmark

BRIAN J. SKINNER
Department of Geology and Geophysics, Yale University, New Haven, Ct. 06520, U.S.A.

Abstract

At low temperatures the tetrahedrite solid solution, Cu_{12+x} $Sb_{4+x}S_{13}$ (Skinner *et al.* 1972, Tatsuka & Morimoto 1973), exsolves into Cu-poor and Cu-rich tetrahedrites. The solvus surface represents one-half of an elliptical paraboloid, open towards Sb-poor compositions, $Cu_{12+x}Sb_4S_{13}$. The highest exsolution temperature, 127.5°C for ~ $Cu_{13}Sb_4S_{13}$, decreases with increasing Sb content and reaches room temperature at $y \sim 0.33$. The coexisting Sb-poor, room-temperature compositions are ~ $Cu_{12.33}Sb_4S_{13}$ (cubic, a 10.32Å) and ~ $Cu_{13.9}Sb_4S_{13}$ (cubic, a 10.45Å). Exsolution tie-lines represent changes in Cu contents, with original Sb contents preserved in both exsolved phases. In pulverized samples, exsolution is nearly strain-free. Single crystals display coherent solvi (perhaps spinodal) owing to parallel orientation of exsolutes with similar structures and a parameters. The linear expansion coefficient of synthetic tetrahedrite between 100 and 250°C is 0.143 x 10^{-3} Å/degree. In tetrahedrite, solid solution is primarily of the interstitial type. The exsolution process is connected with changes in the structural mobility of copper with temperature.

Sommaire

A basse température, la solution solide des tétraédrites, $Cu_{12+x}Sb_{4+y}S_{13}$ (Skinner *et al.* 1972, Tatsuka & Morimoto 1973) se sépare en deux tétraédrites, l'une pauvre et l'autre riche en cuivre. La surface du solvus a la forme d'un demi-paraboloïde elliptique ouvert en direction des compositions pauvres en Sb, $Cu_{12+x}Sb_4S_{13}$. La température maximale de démixtion, 127.5°C pour ~ $Cu_{13}Sb_4S_{13}$, diminue quand la teneur en Sb augmente, jusqu'à atteindre la température ambiante pour $y \sim 0.33$. Les tétraédrites pauvres en Sb à température ambiante sont ~ $Cu_{12.33}Sb_4S_{13}$ (cubique, a 10.32Å) et ~ $Cu_{13.9}Sb_4S_{13}$ (cubique, a 10.45Å). Les phases produites par exsolution diffèrent par leur teneur en cuivre, qui varie tandis que la teneur en Sb originelle reste inchangée. Dans le cas des poudres, la démixtion se produit presque sans déformation de la maille. Les cristaux uniques montrent des solvi cohérents, et peut-être spinodaux, qui résultent de l'orientation parallèle des produits d'exsolution dont les structures sont semblables et les mailles, de même grandeur. Le coefficient d'expansion linéaire de la tétraédrite synthétique entre 100 et 250°C est de 0.143x10^{-3}Å/degré. La solution solide des tétraédrites est surtout du type interstitiel. Le processus de démixtion est lié à des changements de la mobilité structurale des atomes de cuivre, qui varie avec la température.

(Traduit par la Rédaction)

Introduction

The first indications of compositional variations in the tetrahedrite structure type were noticed by Cambi & Elli (1965). They reported that synthetic, arsenic-free tetrahedrites had a compositional field lying along the join Cu_2S–Sb_2S_3 and that two tetrahedrite phases differing slightly in unit-cell edge could coexist over a wide composition range. Cambi & Elli proposed that the two tetrahedrites were dimorphs and suggested that they consisted of a quenched high-temperature form and a coexisting low-temperature modification. Neither their suggestion concerning the compositional field nor the existence of high- and low-temperature tetrahedrites have proven exactly correct, but their observations previewed the results of several later studies.

By determining the phase relations in the system Cu–Sb–S, Skinner *et al.* (1972) discovered that the compositional field of tetrahedrite solid solution is a distorted oval with its longest axis approximately parallel to the join $Cu_{12}Sb_4S_{13}$–$Cu_{14}Sb_4S_{13}$, in disagreement with Cambi & Elli (1965). They also demonstrated that the coexisting tetrahedrites at room temperature, one Cu-rich, the other Cu-poor, arise by exsolution due to the appearance of a solvus along the compositional join. Further study of the exsolved tetrahedrites by Makovicky & Skinner (1972) revealed that the solvus describing the

exsolution must be ternary and not pseudobinary. This meant that in order to understand the exsolution process, the orientation of the solvus tie-lines would be required.

The results of Skinner *et al.* (1972) were confirmed by Tatsuka & Morimoto (1973) who also made a major step forward by delineating the shape of the room-temperature composition field from quenched samples, prepared at 300°C. However, they did not determine the shape of the solvus as a function of temperature, nor the exact room-temperature tie-lines for coexisting tetrahedrites. In the present paper, which amplifies the preliminary results of Makovicky *et al.* (1975), we report on both aspects of the solvus. In the meantime, Tatsuka & Morimoto (1977a) have reported evidence suggesting that the entire tetrahedrite phase field becomes unstable below 250°C, breaking down to famatinite + digenite + antimony. If they are correct, the quenched tetrahedrites and the solvus are actually metastable. We have not been able to confirm or deny the suggestion of Tatsuka & Morimoto, but we would not be surprised if tetrahedrite proves to be yet another example of low-temperature, metastable persistence by an ore mineral.

Experimental Methods

The principal materials used in the present study were charges homogenized and annealed at 400°C during the work reported by Skinner *et al.* (1972). The samples studied were either tetrahedrite solid solutions or multiphase assemblages lying close to tetrahedrite in the system Cu–Sb–S. Most samples were studied by X-ray powder methods, so the charges were first pulverized then separated into two portions; one of these was mounted for room-temperature Guinier photographs.

The a values of all tetrahedrite samples were measured using Guinier-Hägg focusing cameras of the Institute of Mineralogy, University of Copenhagen, using Cu$K\alpha$ radiation, bent quartz crystal monochromators and quartz internal standards. All well-defined reflections of the two exsolved tetrahedrite phases were measured and used for the calculation of the respective cubic lattice parameters a. In extreme cases, where one phase was present in minor amounts, only the strongest reflections could be used.

The other split of the pulverized sample was loaded into thin-walled glass capillaries 0.3 mm in diameter. To ensure tight packing of the powder, the capillaries were shaken in an ultrasonic vibrator. The compacted sulfide powders were topped with crushed glass; the capillaries were evacuated, sealed and then studied in a high-temperature X-ray diffraction camera.

One sample, no. 38, provided us with a unique opportunity. Small, untwinned, single crystals of high-temperature tetrahedrite exsolved on cooling into a mosaic of two untwinned oriented low-temperature tetrahedrites. This fortunate event allowed us also to simultaneously determine the structure of the two coexisting tetrahedrites (Makovicky & Skinner 1976; in prep.). The phases were studied simultaneously by packing a crystal in powdered glass inside a capillary, adding some powdered tetrahedrite of the same composition to serve as a sulfur buffer, and sealing the evacuated capillary. Samples of both powder and mosaic crystals were studied with a Weissenberg camera which was equipped with a heating device consisting of a resistance coil wound and cemented on two ceramic tubes (Fig. 1). The glass capillary lay along the axis of the heating coil and the specimen was irradiated through a 4 mm gap between the two tubes. Temperatures were measured by a thermocouple, also mounted along the tube axis, and positioned so that the

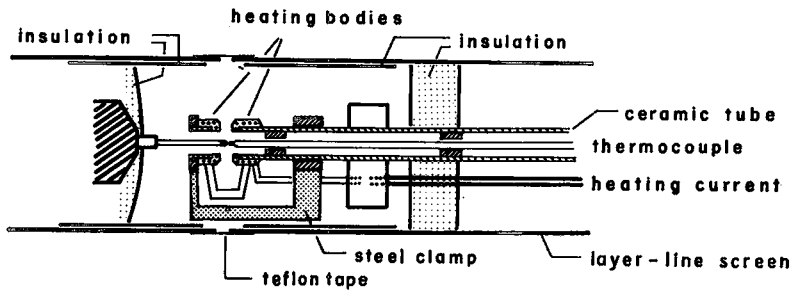

FIG. 1. Heating arrangement for a Weissenberg camera used in annealing experiments on synthetic tetrahedrites. Heat-isolated goniometer head with the crystal in a glass capillary is on the left-hand side. The cylindrical layer-line screen is in position for a zero-layer exposure.

tip of the thermocouple came close to, but did not touch, the sample. Temperatures were calibrated by observing the melting points of benzil (95.5°C), phenacetin (137.5°C) and saccharin (229°C) (Weast 1972). Temperature differences between sample and thermocouple were found to be less than 2°C, and temperature stability during an experiment was ±4°C.

A high-precision split cassette holding one sheet of Weissenberg film was designed, equipped with special clamps to ensure accurate location of the X-ray film. In the case of the powdered samples, the effective radius of the cassette was obtained for each individual film from room-temperature exposures using *a* parameters obtained from room-temperature Guinier photographs of the same samples. A series of exposures at different temperatures, up to 275°C, was then recorded on the same sheet of film. Diffraction angles of the reflections (521), (440) and (611) showing both favorable intensities and large $\Delta\theta$ values for the corresponding reflections of the coexisting tetrahedrites, were measured. For the mosaic crystals the *a* values were calculated using a Nelson & Riley (1945) extrapolation.

Results

Room-temperature composition fields and solvus tie-lines

As seen in Figure 2, the composition field of the tetrahedrite solid solution at elevated temperatures is elongate but bounded in part by curved margins and in part by essentially straight sides. At all temperatures the field is limited on the Sb-poor side by a line joining $Cu_{12}Sb_4S_{13}$ and $Cu_{14}Sb_4S_{13}$. On the Sb-rich side, however, the composition field changes considerably and covers an extensive region expressed by the general formula $Cu_{12+x}Sb_{4+y}S_{13}$. At 300°C, the composition reaches approximately $Cu_{13}Sb_{4.33}S_{13}$ (Tatsuka & Morimoto 1973). Our results and those of Tatsuka & Morimoto overlap at 400°C and above, and differ only in minor details concerning the exact shape of the tetrahedrite composition field. The differences probably reflect small errors accumulated in different stages of the experiments. However, the work of Tatsuka & Morimoto has a special bearing on our study, so the differences must be pointed out (Fig. 2). One difference occurs

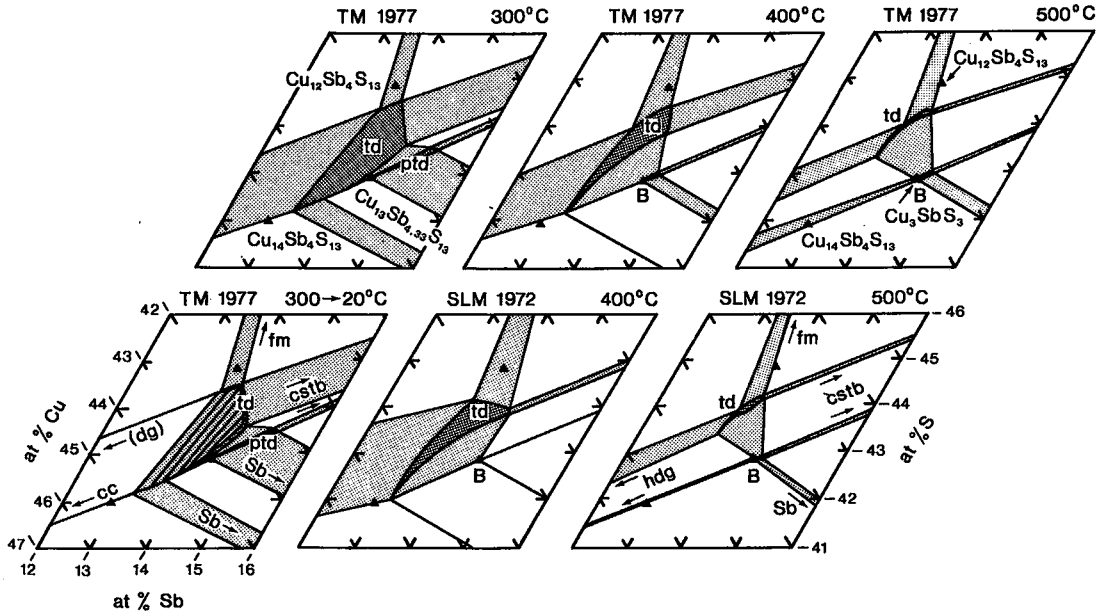

FIG. 2. Comparison of the shape of the tetrahedrite composition field at 300°, 400°, 500°C as determined by Tatsuka & Morimoto (1977a, abbreviated TM) and Skinner *et al.* (1972, abbreviated SLM). The field at 20°C was determined by Tatsuka & Morimoto (1977a) using samples quenched from 300°C. Heavy shading: one-phase fields; light shading: two-phase fields; white: three-phase fields. Symbols: ptd pseudotetrahedrite, td tetrahedrite, B high skinnerite, cstb chalcostibite, fm famatinite, Sb antimony, (h)dg (high) digenite, cc chalcocite. Exsolution tie-lines are indicated for the room-temperature tetrahedrite compositions as given by Tatsuka & Morimoto (1977a). Ideal compositions $Cu_{12}Sb_4S_{13}$, $Cu_{14}Sb_4S_{13}$ and Cu_3SbS_3 (= $Cu_{13}Sb_{4.33}S_{13}$) are indicated by triangles.

at the Cu-poor end of the 400°C field. According to Tatsuka & Morimoto (1977a) the solid solution field extends to slightly more S-rich compositions than reported by Skinner *et al.* (1972). Another difference can be seen in the shape of the field at 500°C (Fig. 2). As previously mentioned, these differences are so small that we place considerable confidence in the experiments of Tatsuka & Morimoto. Where our own data are incomplete, *i.e.*, in the temperature range below 400°C, we have relied heavily on their data.

Tatsuka & Morimoto (1973) observed that below 300°C, the shape of the tetrahedrite composition field thins and moves toward more Sb-rich compositions. Thus, at room temperature they find a very narrow, boomerang-shaped field that rims the Sb-rich edge of the field at 300°C (Fig. 2). The position and shape of the field at room temperature means that most one-phase compositions at high temperatures must exsolve into two phases on cooling. Unfortunately, the composition of the exsolved tetrahedrites cannot be determined by means of electron microprobe studies because they rehomogenize under the electron beam. Thus, we were forced to determine all intergrowth compositions by means of lattice parameters.

All of our starting materials were prepared at 400°C. Because of the shape of the 400°C composition field our charges could not include the most Sb-rich tetrahedrite stable at room temperature; only a few of our samples quenched to single-phase products at room temperature. Therefore, we had to interpret our data by combining the results of Skinner *et al.* (1972) and Tatsuka & Morimoto (1973, 1977a). We started by preparing a best-fitting curve for Tatsuka & Morimoto's unit-cell measurements of one-phase tetrahedrites lying along the

TABLE 1. ROOM TEMPERATURE UNIT CELL PARAMETERS OF THE EXSOLVED PHASES IN SYNTHETIC TETRAHEDRITE SAMPLES

No.	Charge composition atomic %			Temp.	Primary phases	a of exsolved tetrahedrites		No.	Charge composition atomic %			Temp.	Primary phases	a of exsolved tetrahedrites	
	Cu	Sb	S			Cu-poor phase	Cu-rich phase		Cu	Sb	S			Cu-poor phase	Cu-rich phase
1	41.80	13.93	44.27	400°C	td	10.322A	(10.445)A	16	43.00	14.20	42.80	400°C	skin+td	10.326A	-
2	42.19	14.02	43.80	400	td	10.332	(10.420)	17	44.26	12.58	43.16	400	td+fcc	10.320	10.448A
3	42.29	13.75	43.96	400	td	10.321	-	18	40.35	14.19	45.46	600 quench	td+fm cstb	10.318	-
4	42.52	13.74	43.73	300	td	10.315	10.445	19	41.70	14.20	44.10	melt+ 400°C	td+cstb etc.	10.335	10.432
5	42.90	13.50	43.61	400	td	10.321	10.448	20	41.90	14.20	43.90	melt+ 400°C	td+cstb skin	10.335	10.424
6	43.08	13.49	43.43	400	td	10.324	10.449	21	42.16	13.92	43.92	400	td+fcc fm	10.320	10.450
7	37.69	16.69	45.62	400	td+catb	10.326	(10.423)	22	41.90	14.40	43.70	melt+ 400°C	td+cstb skin	10.345	(10.413)
8	41.54	13.96	44.48	400	td+fm	10.321	(10.444)	23	42.50	13.60	43.90	melt+ 500°C	td	10.324	10.448
9	41.76	13.55	44.69	400	td+fm	10.321	10.447	24	42.65	14.46	42.89	400°C	skin (td)	(10.359)	-
10	41.75	13.78	44.47	400	td+fm	10.318	-	25	42.65	14.46	42.89	375°C**	skin (td)	10.338	-
11	42.20	13.53	44.27	300	td+fm (fcc)	10.320	(10.460)	26	43.89	13.48	42.63	melt+ 400°C	td+skin	10.321	10.440
12	42.12	13.73	44.14	400	td+fm	10.319	(10.453)	27	44.10	13.90	42.00	melt+ 400°C	td+skin	(10.343)	10.448
13	42.33	14.10	43.57	400	td+skin	10.340	(10.423)	28	44.70	13.90	41.40	melt+ 400°C	td+Sb (skin)	(10.339)	10.454
14	42.68	14.08	43.04	400	td+skin	10.326	(10.429)	29	45.10	13.90	41.00	melt+ 400°C	Sb+td (skin)	-	10.459
15	43.24	13.09	44.67	300	td+(fcc)	10.317	-	30	45.63	12.59	41.78	melt+ 400°C	td	10.325	10.446

* minor amounts are indicated by parentheses

** hydrothermal run: pressure 2000 bar, 4 M KCl solution

Estimated standard error for the a values is 0.003A (for the values in parentheses 0.006A). All x-ray data were obtained in Guinier-Hägg cameras.

Abbreviations: td-tetrahedrite, skin-skinnerite, fm-famatinite, catb-chalcostibite, fcc-face-centered cubic Cu sulfide

TABLE 2. ROOM TEMPERATURE UNIT CELL PARAMETERS AND EXSOLUTION DATA FOR THE ANNEALED TETRAHEDRITE SAMPLES

Sample No.	Charge composition* atomic %			Formation temp.	Primary phases	Cubic parameters a of exsolved tetrahedrites		Exsolution temperature	Notes on exsolution
	Cu	Sb	S			Cu-poor phase	Cu-rich phase		
31	41.59	14.16	44.25	400°C	td+(fm)	10.318	(10.455)	133±3°C	traces of Cu-rich td
32	45.49	12.60	41.91	400	td+(fcc)	(10.310)	10.449	~25	traces of Cu-poor td
33	44.93	12.58	42.49	400	td+(fcc)	10.317	10.442	113.5±3	
34	43.35	13.30	43.35	400	td+(fcc)	10.317	10.452	127.5±3	solvus crest
35	42.87	13.71	43.42	400	td	10.324	10.438	118±3	solvus crest
36	42.75	13.98	43.25	400	td+skin	10.333	10.431	85.5±3	solvus crest
37**	42.00	14.59	43.41	400	skin+(td)	10.341	10.412	30±10	
38***	42.51	13.61	43.89	400	td	10.323*	10.448*	125±3*	single crystal

Estimated standard error for all the values of a obtained from Guinier photographs is 0.003A.

The a values denoted by * were obtained from calibrated single crystal photographs by extrapolation to $\theta = 90°$ and their est.stand. error is 0.001A.

* see also table 3; ** non-equilibrated run;

*** single crystals from the first annealing of a run with the charge composition $Cu_{12.59}Sb_{4.03}S_{13}$

Exsolution temperatures were obtained on pulverized samples except for the last, single crystal case (*).

boundary of the room-temperature field. We then used the curve to determine compositions of the coexisting room-temperature phases from our own exsolution experiments (Tables 1, 2).

Tie-lines connecting compositions of coexisting tetrahedrites are, within the accuracy of measurement, parallel to the composition join $Cu_{12}Sb_4S_{13}$–$Cu_{14}Sb_4S_{13}$. The tie-lines are well defined in the low-Sb region of the room-temperature solvus, *i.e.*, between the tips of the boomerang-shaped field. At higher Sb contents, however, the tie-lines seem to rotate slightly in an anticlockwise direction. This observation is contrary to the clockwise rotation suggested by Tatsuka & Morimoto (1973, Fig. 3). The discrepancy can be readily explained, however, by comparing our lattice constants for single-phase tetrahedrites with those of Tatsuka & Morimoto (1973). We found excellent agreement in the low-Sb region but a progressive disparity as higher Sb contents are approached until differences as great as 0.01Å are observed for the same composition. If the lattice constant curve is corrected to remove the discrepancy and to fit our data, the apparent rotation disappears and all tie-lines become parallel to the line $Cu_{12}Sb_4S_{13}$–$Cu_{14}Sb_4S_{13}$. Apparently, Tatsuka & Morimoto have also discovered the discrepancy, because Figure 6 of their (1977a) paper shows tie-lines very similar to those we propose here. However, they have yet to discuss the discrepancy between their (1973) and (1977a) papers. We have used the corrected curve (Fig. 9).

For $Cu_{14}Sb_4S_{13}$, a lattice constant of 10.46Å can be extrapolated from both our and Tatsuka & Morimoto's data. In the majority of the exsolved samples the Cu-rich phase only attains the values of 10.44–10.45Å (Table 1; Tatsuka & Morimoto 1973, Table 3). Only two of our multiphase runs (Nos. 28 and 29, Table 1), each of which contains free Sb, gave tetrahedrite compositions close to the ideal Cu-rich end-member; these have a parameters equal to 10.454 and 10.459Å, respectively. Thus, neither composition $Cu_{14}Sb_4S_{13}$, nor $Cu_{12}Sb_4S_{13}$ with a projected lattice parameter of 10.30Å, are reached at room temperature. Our interpretation of the shape of the room-temperature solvus, plotted in terms of the lattice parameter and the variable y in the general tetrahedrite formula $Cu_{12+x}Sb_{4+y}S_{13}$, is shown in Figure 3.

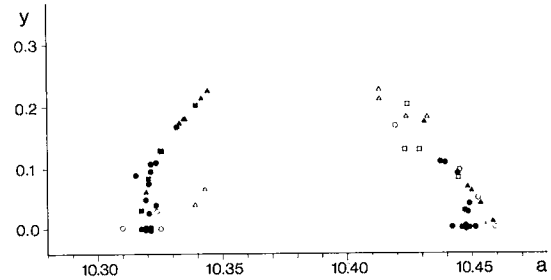

FIG. 3. Room-temperature lattice parameters a (in Å) of exsolved tetrahedrite phases plotted *versus* the y parameter of the homogeneous, high-temperature phase $Cu_{12+x}Sb_{4+y}S_{13}$ from which they quenched. Circles, squares and triangles denote the originally one-, two- and three-phase runs, the latter with indirectly determined y values. Empty symbols indicate trace amounts of the exsolved phase.

Shape of the solvus

Several bulk compositions were selected for powder X-ray studies of tetrahedrite exsolution at temperatures up to 250°C (Table 2). One group of compositions lies close to the crest of the solvus (Fig. 4, first row) and a second group is close to the compositions of the exsolved end-members (Fig. 4, second row).

Sample 38 allowed us to compare the exsolution process in single crystals with that in pulverized samples. For the single-crystal mount, a series of X-ray exposures were taken at fixed temperatures during several heating and cooling cycles. The time allowed for temperature changes between X-ray exposures varied from 10 minutes to two hours. Figure 5 is a composite of several heating and cooling cycles. The direction of the temperature change preceding the given X-ray exposure is indicated by the orientation of the tip of its triangular symbol. The plot indicates that complete reversibility and reproducibility of the exsolution process is possible, without hysteresis, despite the rapidity of the temperature change.

For the pulverized samples, X-ray exposures were taken during the individual steps of the step-wise cooling runs. Two or three such runs were made with each annealed sample (Fig. 4, Table 2). We chose to cool the samples because we expected that the homogenization process on heating might be retarded compared to that in single crystals owing to poorer contacts of the two tetrahedrite phases in the powder.

According to our observations at all temperatures, the exsolved phases in the powders are more completely exsolved than in single crystals of the same composition (as demonstrated for the Sb-poor boundary of the tetrahedrite composition field). This is essentially true at higher temperatures, where very rapid and pronounced exsolution takes place in powdered samples within the first 30°C below

the solvus crest. The difference in lattice constants of the two exsolved phases then changes much less rapidly with falling temperature than is the case for single crystals. Thus, the *a* values of the corresponding exsolved phase in the pulverized sample and in the single-crystal sample

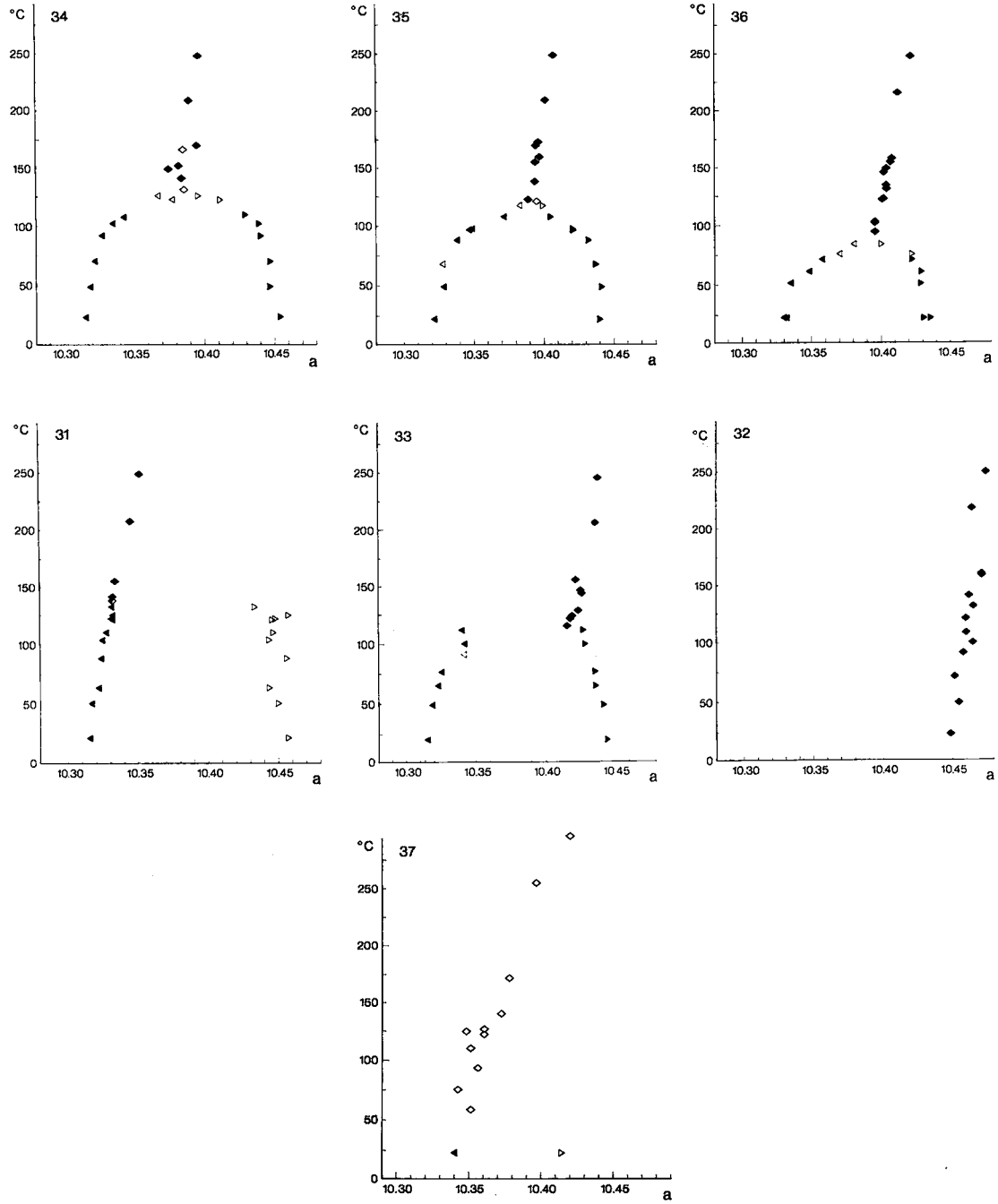

FIG. 4. Unit-cell edges (in Å) of single phases (diamonds) and of coexisting exsolved tetrahedrite phases (triangles) in powdered samples. All results come from multiple cooling runs. Open symbols represent measurements of lower accuracy.

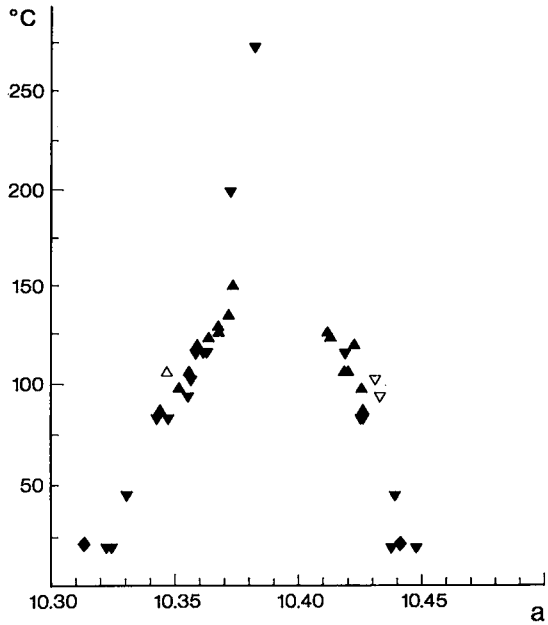

FIG. 5. Unit-cell edges (in Å) of low-temperature exsolution phases in a single crystal of tetrahedrite ~ $Cu_{12.59}Sb_{4.03}S_{13}$ (sample 38). The plot represents a composite of several heating and cooling runs. Orientation of each symbol indicates the temperature change preceding the given measurement. A triangle pointing up means the temperature was raised; an arrow pointing down, the opposite.

converge toward room temperature. The exsolution phenomenon is not composition-dependent, however, because the solvus determined by studying samples situated close to the solvus boundary is identical with that revealed by the centrally situated samples.

The solvus surface, as determined from the heated pulverized samples, is shown in Figure 6. In terms of the lattice parameter *a, corrected for thermal expansion* with help of data from

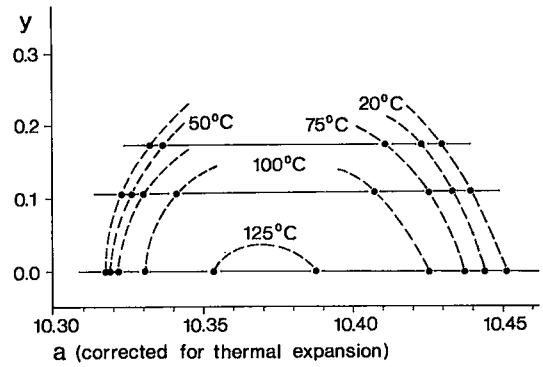

FIG. 6. Shape of the low-temperature tetrahedrite solvus at selected temperatures, in terms of the lattice parameter *a* corrected for thermal expansion, and plotted *versus* the *y* parameter of the original single high-temperature phase $Cu_{12+2y}Sb_{4+y}S_{13}$. Horizontal lines with dots denote the *y* values determined for individual samples.

Table 3, the solvus is half of a distorted elliptical paraboloid, open toward low temperatures and toward Sb-poor compositions. The surface is appreciably asymmetric: the shape is much steeper on the Cu-poor side than on the Cu-rich side. The asymmetry is very pronounced for the compositions poorest in Sb (*y* values below 0.1) and becomes less and less pronounced with increasing contents of Sb.

Thermal expansion

All tetrahedrite runs, including the single-crystal sample, showed a linear thermal expansion above the homogenization (exsolution) temperatures. Least-squares fits to one-phase portions of the heating curves of the pulverized samples (Fig. 4) yielded coefficients of linear expansion for the studied tetrahedrite compositions in the interval between the homogenization temperature and 250°C, from which both the

TABLE 3. THERMAL EXPANSION COEFFICIENTS OF SYNTHETIC TETRAHEDRITES ABOVE THE HOMOGENIZATION TEMPERATURES AND BELOW 250°C

Sample number	Estimated tetrahedrite composition	Linear expansion coefficients A	Bx10⁴	No. of meas. points	Est.stand. error of 1 measurement	Extrapolated $\underline{a}$ at 25°C	Estimated $\underline{a}$ at 200°C	Extrapolated thermal expansion $\frac{V_{200}-V_{25}}{V_{25}}\times 100$
31	$Cu_{\sim 12.3}Sb_{\sim 4.05}S_{13}$	10.3048	(1.8977)	5	.001Å	(10.3101)Å	10.343Å	(0.957)
32	$Cu_{13.9}Sb_{4.0}S_{13}$	10.4473	1.1979	12	.004	10.450	10.471	0.610
33	$Cu_{13.45}Sb_{4.0}S_{13}$	10.3986	1.6631	9	.003	10.403	10.432	0.836
34	$Cu_{13.0}Sb_{4.0}S_{13}$	10.3618	1.3667	7	.006	10.365	10.389	0.699
35	$Cu_{12.85}Sb_{4.1}S_{13}$	10.3735	1.3049	8	.002	10.377	10.400	0.655
38	$Cu_{\sim 12.85}Sb_{4.15}S_{13}$	10.3800	1.6137	13	.002	10.384	10.412	0.820
Average (32-38)			1.4293					0.724

A and B denote coefficients of the linear equation $\underline{a} = A + B\underline{t}$ with the cubic unit cell parameter $\underline{a}$ given in Å and the temperature $\underline{t}$ in °C. Data were obtained from calibrated powder films (see also Table 2).

best-fit lattice constants at 200°C were estimated and the lattice constants of the hypothetical single phases at 25°C were extrapolated (Table 3).

Discussion of Results

Nature and boundaries of tetrahedrite solid solution

Skinner *et al.* (1972) and Tatsuka & Morimoto (1973) suggested that synthetic tetrahedrite compositions could be expressed by the chemical formula $Cu_{12+x}Sb_{4+y}S_{13}$. Their suggestion assumed incorporation of additional Cu and Sb atoms in the crystal structure whereas the number of sulfur atoms per unit cell remained constant. Some evidence has now been accumulated which supports the suggested formula and its assumptions.

Our structure determinations of tetrahedrites (Makovicky & Skinner 1976; in prep.) show that the site occupancies of the sulfur(1) position (nomenclature of Wuensch 1964) are unity in both Cu-poor and Cu-rich tetrahedrites with $y \approx 0$. Also, the occupancy of the S(2) position in the centres of the Cu(2) "spinners" (Wuensch 1964) is unity in Cu-rich phases. The S(2) occupancy in the Cu-poor exsolution phase was determined to be only 0.9. However, this value is within 2 standard errors of full occupancy and might arise from experimental and correlation errors (Makovicky & Skinner, in prep).

The incorporation of up to four atoms of interstitial Cu per unit cell, suggested by an increase in the lattice parameter *a* with increasing Cu content, and by the density measurements of Tatsuka & Morimoto (1973), is now confirmed by the results of our structure determinations. The complexity of this incorporation, with the partial vacating of the tetrahedral Cu(1) position and the highly mobile character of the resulting pool of copper atoms, will be described by Makovicky & Skinner (in prep.). Even the most Cu-rich composition, $Cu_{14}Sb_4S_{13}$, can be understood as a "normal valency" covalent compound, $Cu^{+}{}_{14}Sb^{3+}{}_{4}S_{13}$.

The low-Sb boundary of the tetrahedrite composition field (the join $Cu_{12}Sb_4S_{13}$–$Cu_{14}Sb_4S_{13}$, along which $y = 0$) is apparently sharply defined by the ordered character of the tetrahedrite structure, with 8 Sb atoms per unit cell.

Little is known about the role of additional Sb in the structure of tetrahedrite. Density measurements by Tatsuka & Morimoto (1973), and the existence of an ordered superstructure (pseudotetrahedrite) at compositions close to, and richer in Sb than $Cu_{13}Sb_{4.33}S_{13}$, suggest that excess Sb also might be incorporated in the structure as interstitial atoms. At (and below) 300° and at 355°C, respectively, pseudotetrahedrite and the equivalent (disordered) tetrahedrite extend toward $Cu_{12.39}Sb_{4.54}S_{13}$ (Tatsuka & Morimoto 1977a). Unfortunately, no density measurements are reported for the very Sb-rich compositions. According to Tatsuka & Morimoto (1977a), the decrease of the pseudotetrahedrite lattice constant *a* with increasing Sb-content along the join Cu_2S–Sb_2S_3 is much less pronounced than for normal tetrahedrite in the interval $Cu_{14}Sb_4S_{13}$–Cu_3SbS_3.

The boundary of the solid-solution field between the compositions $Cu_{14}Sb_4S_{13}$ and $Cu_{13}Sb_{4.33}S_{13}$ (or the corresponding portion of the room-temperature solid solution) is essentially straight and within accuracy of measurement displays a small linear change of *a vs* composition. The change apparently represents an exchange of the interstitial metal atoms, so that $Cu^{+} \rightleftarrows \frac{1}{3}\ Sb^{3+}$. The compositions between $Cu_{13}Sb_{4.33}S_{13}$ and $Cu_{12.39}Sb_{4.54}S_{13}$ probably arise by an extension of the same Sb-substitution mechanism to still lower contents of interstitial copper. The hypothetical limiting case, $Cu_{12}Sb_{4.67}S_{13}$, has not been synthesized. Compositions richer in metals than the "normal valency" compositions were not observed.

Where the tetrahedrite composition field lies adjacent to chalcostibite, at 350°C, the line limiting tetrahedrite compositions connects $Cu_{12}Sb_4S_{13}$ to the most Sb-rich pseudotetrahedrite composition (Tatsuka & Morimoto 1977a). However, all the Sb-rich composition limits recede quickly with increasing temperature (Fig. 2). This compositional change is caused by the increasing stability of high skinnerite (phase B, Fig. 2) at high temperatures (Skinner *et al.* 1972, Karup-Møller & Makovicky 1974). Compared with tetrahedrite, skinnerite has a "Sb-rich" composition of Cu_3SbS_3.

The last portion of the tetrahedrite composition field represents a short, nearly linear segment that lies adjacent to the "ideal tetrahedrite" composition, $Cu_{12}Sb_4S_{13}$. The boundary follows closely compositions with a nearly constant value of *a*, but not lines of simple valency compensations. Chemically this boundary is difficult to characterize. Because of the way the field-boundary position changes with temperature, neither the studies of Skinner *et al.* (1972) nor those of Tatsuka & Morimoto (1973) yielded pure tetrahedrite for the compositions measured for the room-temperature boundary (*cf.*, Tatsuka & Morimoto 1973, Table 3).

At room-temperature, the composition of the tetrahedrite poorest in Cu having $y = 0$ is

estimated to be $Cu_{12.33}Sb_4S_{13}$. This tetrahedrite has a unit-cell edge of 10.319Å. The compositions richest in Sb along the above boundary, with $y \approx 0.1$, have a equal to approximately 10.321Å. The boundary suggests that some interatomic distances in the structure might have reached their minimum, thus preventing further contraction of the structure and the concurrent decrease in copper content. The determination of the structure of $Cu_{12.33}Sb_4S_{13}$ (Makovicky & Skinner, in prep.) shows that the likely explanation might be the already extensive compression of S(1)–S(1) distances in the "spinners" and in the tetrahedral framework of this compound. The growing disparity between the sturdy $[SbS_3]$ coordination pyramids and progressively smaller $[Cu(1)S_4]$ tetrahedra is unlikely to represent the principal explanation of the compositional boundary, because a similar low-Cu compositional limit occurs in synthetic tennantite, in which much smaller $[AsS_3]$ pyramids occur (Maske & Skinner 1971). In the substituted natural and synthetic tetrahedrites, $Cu^{+}{}_{10}(Fe,Zn,Cu)^{2+}{}_2Sb_4S_{13}$, the average sizes of tetrahedra stay sufficiently large, and the above limitations do not come into question.

An added, or alternative, reason, also absent in the above substituted tetrahedrites, might be the energetical advantage of a lower Cu^{2+}/Cu^{+} ratio filling the valency band not by the combination $Cu^{+}{}_{10}Cu^{2+}{}_2Sb^{3+}{}_4S_{13}$, but by a slightly more Cu-rich combination $Cu^{+}{}_{10+2x}Cu^{2+}{}_{2-x}Sb^{3+}{}_4S_{13}$. The observed unsubstituted composition poorest in Cu is $\sim Cu^{+}{}_{10.66}Cu^{2+}{}_{1.66}Sb_4S_{13}$. The structure analysis (Makovicky & Skinner, in prep.) shows that the incorporation of additional copper even in this case is connected with partial vacating of the tetrahedral Cu(1) position. The Cu^{2+}/Cu^{+} ratio of this tetrahedrite is 0.156. It is remarkably close to the Cu^{2+}/Cu^{+} ratio of the digenite poorest in Cu, $Cu_{1.765}$ S, equal to 0.152, or of the occasionally observed digenite composition $Cu_{1.75}$ S (0.167). The latter also represents the composition of the low-temperature phase anilite (Morimoto & Koto 1970, Barton 1973). The full meaning of this coincidence in the Cu^{2+}/Cu^{+} values is not clear. All these phases represent defect stuffed *ccp* structures of some sort, and the Cu^{2+}/Cu^{+} ratios also indicate certain minimal Cu/*(relevant portion of)*S ratios or perhaps, the minimal stable atomic concentration per available copper positions.

The tetrahedrite composition richest in Sb on the boundary with minimal a values can roughly be estimated as $\sim Cu_{12.18}Sb_{4.09}S_{13}$; it has a Cu^{2+}/Cu^{+} ratio of 0.144 (*i.e.*, $Cu_{1.776}$S). Owing to the difficulties described in estimating the composition of the Cu-poor field boundary, the reliability of this ratio is low. Similar considerations of structure or charge balance or both might also apply to the Cu-rich tetrahedrites that do not attain the most Cu-rich composition, $Cu_{14}Sb_4S_{13}$.

Opinions are divided concerning the presence of Cu-rich (metal-rich) tetrahedrites in nature, where Fe, Zn and other divalent metals substituting for copper are readily available. From microprobe analyses, Springer (1969) and Charlat & Levy (1974) favor the $Me_{12}Sb_4S_{13}$ composition, whereas Nash (1975) favors a metal-enriched composition. For synthetic substituted samples Cambi *et al.* (1965) and Tatsuka & Morimoto (1977b) describe metal-enriched compositions but Hall (1972) suggests only compositions with $\Sigma Me = 12$. We cannot yet add to or resolve the speculations, but we continue to work on the problem.

The exsolution process

The general trend of the exsolution tie-lines at room temperature, parallel to the $Cu_{12}Sb_4S_{13}$–$Cu_{14}Sb_4S_{13}$ join, indicates that the two exsolved phases possess the same Sb content and that exsolution proceeds by diffusion of copper atoms (*cf.*, Tatsuka & Morimoto 1973). These conclusions are valid for quenched and cooled tetrahedrites measured either immediately or long (up to 3 years) after annealing. This can be compared with the ready diffusion of copper atoms observed in copper sulfides (Buerger & Wuensch 1963, Sadanaga *et al.* 1975) and in copper-rich sulfosalts (Makovicky *et al.* 1975, Makovicky & Skinner 1972, 1975). In all these compounds, the copper atoms were found to change from a stationary to a mobile state at relatively low temperatures, from 90° to 160°C.

Changes in the Sb content of tetrahedrite will necessarily be complicated by the highly asymmetric coordination of Sb^{3+} in sulfides, with its lone pair of electrons (long Sb–S distances) structurally accommodated on one side of its coordination polyhedron. Thus we may reasonably expect that the distribution of additional Sb atoms in the high-temperature structure will in principle be inherited by both of the exsolved low-temperature phases, *i.e.*, the dissociation will only change the Cu contents of the daughter phases.

In the chemically similar high skinnerite, Cu_3SbS_3, the isolated $[SbS_3]$ groups were found to be stationary in a structure determination performed at 170°C (Makovicky & Skinner, in prep.).

The temperature of the crest of the solvus

(127°C) for Sb-poor tetrahedrites ($y = 0$) is close to the temperature of the low-to-high phase transformation in skinnerite, Cu_3SbS_3, and in wittichenite, Cu_3BiS_3, 122°C and 118°C, respectively (Makovicky *et al.* 1975, Karup-Møller & Makovicky 1974). In these two sulfosalts, a marked increase in crystallographic symmetry is observed in the high-temperature form, indicating a qualitative (stationary→(partly) mobile) change in the state of copper upon transformation. The observation of domain structure in the high-temperature form of Cu_3BiS_3 (Makovicky & Skinner 1975) within the first 50°C above the phase transition shows that the "melting" (van Gool 1974) of the copper array only becomes complete after a considerable temperature rise. It also involves anomalies in thermal expansion.

For synthetic tetrahedrites there are no sudden changes in X-ray intensities, no changes in symmetry and no thermal expansion anomalies in either of the exsolved phases. Thus, the mobility (*i.e.*, disordering) and/or the number of copper atoms involved in the exsolution/homogenization processes seem to increase steadily from (below) room temperature upward, and to become substantial within about 30°C below the homogenization temperature. Introduction of "additional" antimony reduces compositional and dimensional difference between the two exsolved phases. Thus, the temperature of the solvus crest drops, and at room temperature, the solid solution field closes on the Sb-rich side.

Although synthetic tennantite shows a large compositional field $Cu_{12+x}As_{4+y}S_{13}$ similar to that of tetrahedrite (Maske & Skinner 1971), the low-temperature exsolution phenomenon is not observed. Even small amounts of arsenic (above 8 mol. % of the tennantite component) can suppress the exsolution processes in tetrahedrites (Luce *et al.* 1977). Apparently the changes in structural geometry caused by the introduction of much larger $[SbS_3]$ pyramids in place of $[AsS_3]$ pyramids are such that with decreasing mobility of copper, as temperature is lowered, only the Cu-poor (rather empty with respect to "additional Cu") and the Cu-rich (nearly fully "stuffed" with "additional Cu") tetrahedrite compositions remain stable.

The shape of the solvus

The two exsolved tetrahedrite phases have similar crystal structures, parallel crystallographic orientation and, at least at the beginning of the exsolution process, very similar lattice constants and *coherent* phase boundaries. With

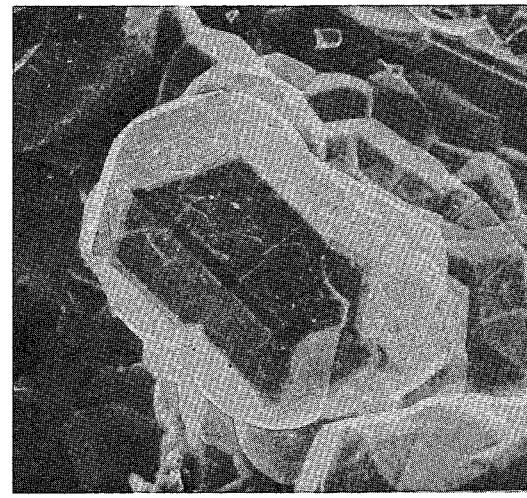

FIG. 7. Scanning electron microscope photograph of a synthetic tetrahedrite aggregate (specimen 38). Low-temperature exsolution disrupted the aggregate with a net of irregular cracks. Magnification 227×.

continuing exsolution, differences in lattice constants increase and the strained aggregates become disrupted by irregular cracks (Fig. 7). The cracks partly follow the irregular boundaries between the randomly arranged micrograins of the two exsolved tetrahedrite phases (Fig. 8). Unfortunately, details of composition and crystallographic homogeneity of the optically individualized exsolved grains (Fig. 8) could not

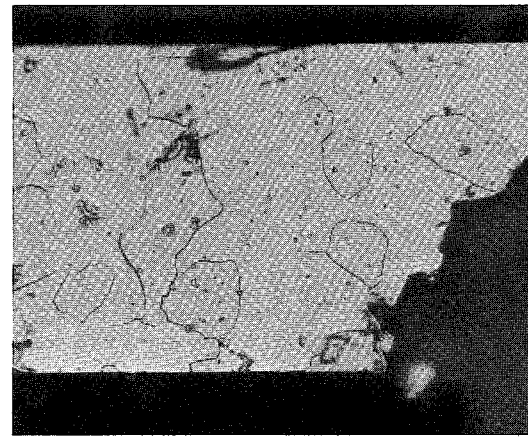

FIG. 8. Microphotograph of the surface of an exsolved synthetic tetrahedrite crystal (specimen 38), elongate parallel to [111]. Darker grains presumably represent the phase richer in Cu, the lighter matrix the Cu-poor phase. Magnification 380×.

be examined due to their small size as well as to the rehomogenization of tetrahedrite under the microprobe beam. Where one of the exsolved phases is present in small amounts, its single-crystal reflections display small "tails" due to strain.

In the minute grains of the pulverized specimens exsolution probably produces a minimum of coherent boundaries, so that the resulting phases are primarily bounded by free space. Thus, the situation in the powder, essentially strain-free, leads to maximal exsolution. Furthermore, the dislocations introduced upon thorough grinding apparently facilitate nucleation and non-coherent exsolution of the resulting phases. The diffraction lines of the two exsolved phases are always sharp and well-defined.

Thus, the two solvi, one obtained on single crystals (sample 38, Fig. 5) and the other on the pulverized samples (*e.g.*, sample 34, Fig. 4 top row) most likely approximate a coherent and a strain-free solvus, respectively. The coherency is partly lost on further cooling, owing to the development of cracks within specimens, and at lower temperatures the solvus obtained on single crystals approaches the solvus from powders. No significant lowering of the crest of the coherent curve against that of the strain-free solvus could be observed. We cannot comment on this point because none of the elastic constants involved in this temperature difference (Cahn 1962) has been measured for tetrahedrite (Birch 1966).

To a first approximation the crystal structures of the tetrahedrites studied should consist, at elevated temperatures, of a framework of stationary atoms and a mobile, "liquid" pool (van Gool 1974) of copper atoms with a high diffusion coefficient. This situation seems to be well-suited for the formation of large-scale wave-like compositional fluctuations (concentrations of copper atoms) in the original phase in the vicinity of the solvus (Cahn 1962, 1968), in a way similar to some framework silicates (Aaronson *et al.* 1974). This might result in spinodal decomposition of the high-temperature phase and the observed coherent curve might then be, at least in its upper parts, close to a coherent spinodal.

Due to the high diffusion coefficient of copper and excessive strains at lower temperatures, the spinodal will not be frozen on quenching; irregular semi-coherent grains of one phase in

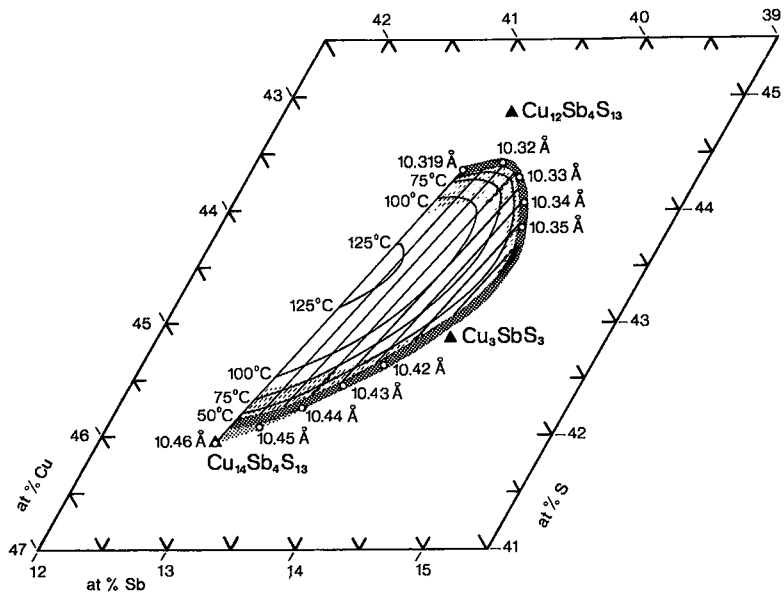

FIG. 9. Tentative plot of the composition field of the synthetic tetrahedrite solid solution at room temperature, and of the slope of the low-temperature solvus in the Cu–Sb–S compositional diagram. Compositions are given in atomic percent. Lattice parameters *a* are indicated for room-temperature compositions. Lighter area indicates rarely encountered compositions. Hatched areas indicate the room-temperature compositions of coherent and semi-coherent exsolved phases.

the other will quickly nucleate and grow. No superstructure due to spinodal fluctuations was observed on the single-crystal X-ray photographs taken near the solvus crest.

Where one of the exsolved phases is present in minimal amounts, (*i.e.*, in few, widely spaced grains), even powdered samples will approximate coherent exsolution. Thus, the composition of the minor phase will follow a coherent solvus; its lattice parameter *a* was found to fall short of the expected values by up to 0.02Å (Fig. 3 and Table 1). The amount of strain per unit volume of the major phase will be minimal and the latter will proceed to the strain-free exsolution compositions.

The tentative projection of the low-temperature, essentially strain-free solvus, and of the room-temperature compositional field of tetrahedrite onto the compositional plot Cu–Sb–S is given in Figure 9. For the interpretation of the solvus, we assumed linear dependence of the lattice parameter *a* on the value of the coefficient *x* in the formula $Cu_{12+x}Sb_{4+y}S_{13}$. The results show a much steeper slope of the solvus for Cu- and Sb-poor compositions of the composition field. The asymmetry of the solvus can be explained by the same arguments as used for the explanation of the position and shape of the Cu-poor boundary of the tetrahedrite composition field in the foregoing section. Should the change of *a* with *x* become nonlinear in the regions poorest in Cu, the shape of the tetrahedrite solvus in the Cu–Sb–S diagram will be less asymmetric.

The shape of the solvus both in Figures 6 and 9 does not support rotation of the exsolution tie-lines at higher temperatures compared to the room-temperature situation.

Acknowledgments

Assistance of Mrs. A. Christensen in the X-ray work, of Mr. F. D. Luce in sample preparation, and of Mrs. T. Kock, M. Hornstrup and R. Larsen in the preparation of the manuscript is acknowledged. Research has been supported by the National Science Foundation, U.S.A. (grant GA-4142) and by the State Research Council, Denmark (grant 511-3594).

References

Aaronson, H. I., Lorimer, G. W., Champness, P. E. & Spooner, E. T. C. (1974): On differences between phase transformations (exsolution) in metals and silicates. *Chem. Geology* **14**, 75-80.

Barton, P. B., Jr. (1973): Solid solutions in the system Cu–Fe–S. I. The Cu–S and CuFe–S joins. *Econ. Geol.* **68**, 455-465.

Birch, F. (1966): Compressibility; elastic constants. *In* Handbook of Physical Constants (S.P. Clark, Jr., ed.). *Geol. Soc. Amer. Mem.* **97**.

Buerger, M. J. & Wuensch, B. J. (1963): Distribution of atoms in high-chalcocite, Cu_2S. *Science* **141**, 276-277.

Cahn, J. W. (1962): Coherent fluctuations and nucleation in isotropic solids. *Acta Met.* **10**, 907-913.

——— (1968): Spinodal decomposition *Met. Soc. A.I.M.E. Trans.* **242**, 166-180.

Cambi, L. & Elli, M. (1965): Processi idrotermali. Sintesi di solfosali da ossidi di metalli e metalloidi. II. Cuprosolfoantimoniti. *Chim. Ind.* **47**, 136-147.

———, ——— & Tangerini, I. (1965): Processi idrotermali. IV. Tetraedriti sostituite. *Chim. Ind.* **47**, 703-715.

Charlat, M. & Levy, C. (1974): Substitutions multiples dans la série tennantite–tétraédrite. *Soc. franç. Minéral. Crist. Bull.* **97**, 241-250.

Hall, A. J. (1972): Substitution of Cu by Zn, Fe and Ag in synthetic tetrahedrite, $Cu_{12}Sb_4S_{13}$. *Soc. franç. Minéral. Crist. Bull.* **95**, 583-594.

Karup–Møller, S. & Makovicky, E. (1974): Skinnerite, Cu_3SbS_3, a new sulfosalt from the Ilímaussaq alkaline intrusion, South Greenland. *Amer. Mineral.* **59**, 889-895.

Luce, F. D., Tuttle, C. L. & Skinner, B. J. (1977): Studies of sulfosalts of copper. V. Phases and phase relations in the system Cu–Sb–As–S between 350° and 500°C. *Econ. Geol.* **72**, 271-289.

Makovicky, E., Makovicky, M. & Skinner, B. J. (1975): Crystallography and phase transitions of copper-rich sulphosalts between 25°C and 170°C. *Fortschr. Mineral.* **53** (Bh. 1), 52 (Abstr.).

——— & Skinner, B. J. (1972): Crystallography of Cu_3SbS_3. *Amer. Cryst. Assoc. Meet.*, 61 (Abstr.).

——— & ——— (1975): On crystallography and structures of copper-rich sulphosalts between 25°–170°C. *Acta Cryst.* **A31**, S65 (Abstr.).

——— & ——— (1976): Crystal structures of synthetic tetrahedrites $Cu_{12+\delta}Sb_4S_{13}$ and $Cu_{14-\delta}Sb_4S_{13}$. *Neues Jahrb. Mineral. Monatsh.*, 141-143.

Maske, S. & ——— (1971): Studies of the sulfosalts of copper. I. Phases and phase relations in the system Cu–As–S. *Econ. Geol.* **66**, 901-918.

Morimoto, N. & Koto, K. (1970): Phase relations of the Cu-S system at low temperatures: stability of anilite. *Amer. Mineral.* **55**, 106-117.

Nash, J. T. (1975): Geochemical studies in the Park City district. II. Sulfide mineralogy and minor-

element chemistry, Mayflower mine. *Econ. Geol.* **70**, 1038-1049.

NELSON, J. B. & RILEY, D. P. (1945): An experimental investigation of extrapolation methods in the derivation of accurate unit-cell dimensions of crystals. *Phys. Soc. London Proc.* **57**, 160-177.

SADANAGA, R., OHMASA, M. & MORIMOTO, N. (1965): On the statistical distribution of copper ions in the structure of β-chalcocite. *Mineral. J. (Japan)* **4**, 275-290.

SKINNER, B. J., LUCE, F. D. & MAKOVICKY, E. (1972): Studies of the sulfosalts of copper. III. Phases and phase relations in the system Cu–Sb–S. *Econ. Geol.* **67**, 924-938.

SPRINGER, G. (1969): Electron probe analyses of tetrahedrite. *Neues Jahrb. Mineral. Monatsh.* 24-32.

TATSUKA, K. & MORIMOTO, N. (1973): Composition variation and polymorphism of tetrahedrite in the Cu–Sb–S system below 400°C. *Amer. Mineral.* **58**, 425-434.

——— & ——— (1977a): Tetrahedrite stability relations in the Cu–Sb–S system. *Econ. Geol.* **72**, 258-270.

——— & ——— (1977b): Tetrahedrite stability relations in the Cu–Fe–Sb–S system. *Amer. Mineral.* **62**, 1101-1109.

VAN GOOL, W. (1974): Fast ion conduction. *Ann. Rev. Mat. Sci.* **4**, 311-335.

WEAST, R. C., ed. (1972): *Handbook of Chemistry and Physics*, 52nd ed. The Chemical Rubber Co., Cleveland.

WUENSCH, B. J. (1964): The crystal structure of tetrahedrite, $Cu_{12}Sb_4S_{13}$. *Z. Krist.* **119**, 437-453.

Received December 1977; revised manuscript accepted April 1978.